PSM
Biological Research

Research Article 2026 | Volume 11 | Issue 1 | 90-104

Open Access

Article Information

Received: July 27, 2026

Accepted: September 7, 2026

Published: September 21, 2026

Authors' Contribution
IA designed the study, and developed the HYDRUS 2D model, ZAK prepared the original manuscript; AAA conducted the experiments; PJP collected the data; MASA supervised the study, IAS contributed to interpretation of results and manuscript review; all authors approved the final version of the manuscript.

How to cite
Arshad, I., Ali, A.A., AlMansoori, A.M.S., Philip, P.J., Shaikh, I.A., Khan, Z.A., 2026. Experimental Assessment of Soil Wetting Geometry under Point Source Drip Irrigation Using HYDRUS-2D Simulation. PSM Biol. Res., 11(1): 90-104.

***Correspondence**
Imran Arshad
Email: engr_imran1985@yahoo.com

Experimental Assessment of Soil Wetting Geometry under Point Source Drip Irrigation Using HYDRUS-2D Simulation

Imran Arshad[1*], Ali Ahmed Ali[2], Mubarak Ahmed Saleh AlMansoori[3], Phiji Jacob Philip[4], Irfan Ahmad Shaikh[5], Zaheer Ahmed Khan[6]

[1]Star Services LLC, Ghayathi Extension Center (ADAFSA Project), Ghayathi City, Abu Dhabi, United Arab Emirates.
[2]Ghayathi Extension Center, Abu Dhabi Agriculture and Food Safety Authority (ADAFSA), Ghayathi City, Abu Dhabi, United Arab Emirates.
[3]Department of Research and Development AlDhafra Region, Abu Dhabi Agriculture and Food Safety Authority (ADAFSA), Madinat Zayed City, Abu Dhabi, United Arab Emirates.
[4]Star Services LLC, Madinat Zayed Extension Center (ADAFSA Project), Madinat Zayed City, Abu Dhabi, United Arab Emirates.
[5]Department of Irrigation and Drainage, [6]Department of Farm Structures and Postharvest Engineering, Faculty of Agricultural Engineering and Technology, Sindh Agricultural University, Tandojam, Sindh, Pakistan.

Abstract:
Numerical modeling of movement of water through the soil can effectively estimate the wetting pattern below drip emitters and analyse the irrigation design parameters in arid soils. This study simulated the time-based variations of the wetting volume below the surface point source emitter using HYDRUS-2D software. The two-dimensional model was utilized to evaluate the wetting pattern in a loamy sand soil of Ghayathi, Abu Dhabi, United Arab Emirates, by considering an experiment conducted on the non-cropped soil with a discharge of 2 L h^{-1} for 180 min. The irrigation experiment was performed at the surface of the soil with 15 min intervals, and surface wetted radius, surface diameter, and maximum depth were determined. The soil hydraulic parameters were found at 0-75 cm depth with 15 cm intervals. The van Genuchten-Mualem model parameters were calculated as $\theta_r = 0.043$, $\theta_s = 0.368$, $\alpha = 0.069$ cm^{-1}, $n = 1.73$, and $K_s = 1.56$ cm h^{-1} on the average of the five-layer of the soil. The simulation process involved in the 2-D model of 70 × 100 cm covered the domain by dividing it into 1,543 nodes and 3,084 triangular finite elements. The point source emitter was assumed a constant-flux boundary condition. It was observed that the wetting volume increased during the irrigation process with 12.0 - 24.0 cm of surface wetted radius and 16.0 - 74.0 cm of wetting depth. The simulated values were found to be 11.38 - 22.03 cm and 16.45 - 69.40 cm of surface wetted radius and wetting depth with the irrigation time of 180 min. Additionally, the good performance of the model was evaluated based on RMSE (1.07 cm for the wetted radius; 3.19 cm for the wetting depth), model efficiency (91.80% for the radius; 96.62% for the depth), R^2 (> 0.98), which slightly underestimated the experimental measurements at long irrigation durations. The accuracy of the HYDRUS-2D model was verified by plotting a log-log regression of observed and simulated wetting dimensions for all durations. Since the slope of the line is close to one and the model efficiency is greater than 90%, there is no evidence of scale dependence. Hence, these results confirm that HYDRUS-2D model satisfactorily describes the geometry of the wetted volume under the point source drip irrigation.
Keywords: Drip irrigation, HYDRUS-2D software, loamy sand, point source, soil water movement, wetting front, model validation.

INTRODUCTION

Drip irrigation technology allows for applying water at low pressure rates to small cores of soil and can be highly efficient in terms of control of the water distribution in water limited environments. However, its hydraulic performance cannot be considered when taken in isolation when analyzing the ability of a drip system to supply water to plants. It is essential to ensure that the size and shape of the wetted volume are adequate for the root system geometry, emitter spacing, duration of irrigation, and the hydraulic characteristics of the medium. The inadequate pattern of wetting may lead to either insufficient soil moisture due to poor contact with the root system or deep percolation loss of water below the root zone. The movement of water below a point source emitter is controlled by capillary forces, gravity, the content of water in the soil, the discharge from an emitter, and the hydraulic properties of the soil (Cook *et al.,* 2003). In the initial phase of irrigation, capillary forces cause water to spread horizontally and vertically from a point emitter. However, with time, gravity increasingly dominates over capillary forces, which is particularly evident in coarse textured soils with large pores, moderate to high hydraulic conductivity, and low total water content. As a result, the shape of the wetted volume transforms from a shallow hemisphere into an elongated bulb (Schwartzman and Zur, 1986).

Direct measurements of wetting fronts are informative but time consuming, laborious, and challenging to make below the surface of the soil. Numerical models offer one way to simulate time-variable water contents for a range of conditions. HYDRUS-2D solves the Richards equation for the domain of variable saturation using the finite element method. The soil hydraulic functions have typically been described using the van Genuchten-Mualem model (Richards, 1931; Mualem, 1976; van Genuchten, 1980; Šimůnek *et al.,* 2016). Previous works showed the model's ability to predict measured field patterns of wetting fronts for surface and subsurface drip irrigation (Skaggs *et al.,* 2004; Kandelous and Šimůnek, 2010). However, model performance depends on the accuracy of the hydraulic parameters, the approximation of the boundary condition at the emitter location, and the specific algorithm for determining the advance of the wetting front. In arid agricultural areas, loamy sandy soils are widespread and challenging to manage due to the rapid downward movement of water below the root zone (Cote *et al.,* 2003). Numerical experiments demonstrated that the texture, discharge rate, and initial moisture content were the most influential parameters on the infiltration process in such soils (Naglič *et al.,* 2014). However, empirical and dimensional analysis also showed that irrigation amount and saturated hydraulic conductivity were the most critical factors influencing wetting front characteristics (Al-Ogaidi *et al.,* 2016; Fan *et al.,* 2023). Therefore, it is essential to validate the model in local conditions to ensure that it properly captures the relationship between the input parameters and irrigation performance before using HYDRUS-2D to determine optimal emitter spacing and schedule irrigation (Zur, 1996).

The objective of this study was to evaluate HYDRUS-2D predictions of surface and subsurface wetting-front development below a 2 L h^{-1} surface emitter in a loamy sand profile under arid conditions. Specifically, the study aimed to: (i) to find out the time-based variation of observed radial and vertical wetting front dimensions was characterized; (ii) to simulate the two-dimensional water content profiles; (iii) to determine the model accuracy using the mean error, root mean square error, model efficiency, maximum absolute relative error, and coefficient of determination; and (iv) interpret the implications for drip-irrigation design and operation in comparable coarse-textured soils.

MATERIALS AND METHODS

Study location and experimental overview

A field experiment was conducted on an arid loamy sand soil at Ghayathi in the Aldhafra region of Abu Dhabi, United Arab Emirates. The test represented infiltration from a single surface source into bare soil with root water uptake being set to zero and evaporation being neglected due to the relatively short duration of the irrigation events and the groundwater was used as the water source. Water was applied continuously at 2 Lh^{-1} for 180 min (total applied volume = 6 litres) at 1 bar operating pressure respectively. Surface wetting and maximum vertical advance were recorded every 15 min.

Soil hydraulic characterization

The soil was sampled at five depths from 0 to 75 cm. The soil bulk density increased with depth, whereas the saturated water content and the van Genuchten α and n parameters and unsaturated hydraulic conductivity decreased with depth. Table 1 summarizes the soil physical properties obtained in the laboratory.

Theoretical considerations

Formation of a wetted soil volume under a surface point source of drip irrigation is an outcome of water infiltration into the porous medium. Redistribution of applied water occurs both laterally and vertically from an emission point creating a wetting pattern, commonly known as the wetting bulb. The shape and time development of this pattern is controlled by soil hydraulic properties, intensity and duration of water application as well as gravity.

At the initial stage of irrigation, the flow of water is mainly controlled by the gradients of matric potentials in the vicinity of the emitter resulting in significant lateral as well as vertical advance of soil water. With an increase in the duration of irrigation, and consequently, the size of the wetted area, the role of gravity increases, especially for coarse textured soils. Due to this, the advance of water becomes deeper and more vertical than horizontal, with an increase in the time of irrigation.

Table 1. Layer wise hydraulic properties of the arid loamy sand soil profile.

Layer	Depth (cm)	Bulk density	Residual water content	Saturated water content	Van Genuchten shape parameters	Saturated hydraulic conductivity
		($g\,cm^{-3}$)	θr ($cm^3\,cm^{-3}$)	θs ($cm^3\,cm^{-3}$)	α (cm^{-1})	n
1	0–15	1.55	0.045	0.385	0.078	1.86
2	15–30	1.60	0.045	0.375	0.073	1.79
3	30–45	1.63	0.043	0.365	0.068	1.72
4	45–60	1.66	0.042	0.360	0.064	1.67
5	60–75	1.68	0.041	0.355	0.060	1.62

For the HYDRUS-2D simulation, depth averaged parameters were soil bulk density= 1.63, θr = 0.043, θs = 0.368, α = 0.069 cm^{-1}, n = 1.73, and Ks = 1.56 $cm\,h^{-1}$.

Governing Equation for Soil Water Movement

The movement of water in the soil under the point source drip irrigation is taking place under the variably saturated conditions and can be described by the Richards equation that combines the Darcy's law and continuity equation as follows:

$$\frac{\partial\theta(h)}{\partial t}=\frac{\partial}{\partial x}\left[K(h)\frac{\partial h}{\partial x}\right]+\frac{\partial}{\partial z}\left[K(h)\left(\frac{\partial h}{\partial z}+1\right)\right]-S(h)$$

Where;

$\theta(h)$ = volumetric water content of the soil ($cm^3\,cm^{-3}$)

h= soil water pressure head (cm)

$K(h)$ = unsaturated hydraulic conductivity as a function of pressure head ($cm\,h^{-1}$)

x= horizontal coordinate (cm)

z= vertical coordinate, positive upward (cm)

t= time (h)

$S(h)=0$= sink term representing root water uptake ($cm^3\,cm^{-3}\,h^{-1}$).

However, the root water uptake as well as the surface evaporation has been neglected in the current study.

Soil Hydraulic Relationships

The hydraulic function of the soil is described by continuous water retention and hydraulic conductivity relationships (van Genuchten, 1980). The soil water retention curve was described using the following equation:

$$\theta(h) = \theta_r + \frac{\theta_s - \theta_r}{[1 + (\alpha \mid h \mid)^n]^m} (h < 0)$$

Where;

$\theta(h)$ = volumetric water content at pressure head h(cm³ cm⁻³)

θ_r= residual volumetric water content (cm³ cm⁻³)

θ_s= saturated volumetric water content (cm³ cm⁻³)

h= soil water pressure head (cm)

α= inverse of the air entry pressure (cm⁻¹), related to pore size distribution

n= dimensionless empirical shape parameter controlling the slope of the retention curve

$m = (1 - \frac{1}{n})$ = shape parameter

The unsaturated hydraulic conductivity is expressed by Mualem-van Genuchten model:

$$K(h) = K_s S_e^l \left[1 - \left(1 - S_e^{1/m}\right)^m\right]^2$$

Where;

$K(h)$ = unsaturated hydraulic conductivity at pressure head h(cm h⁻¹)

K_s= saturated hydraulic conductivity (cm h⁻¹)

$S_e = \frac{\theta - \theta_r}{\theta_s - \theta_r}$ = effective saturation,

l = pore connectivity (tortuosity) parameter,

$m = (1 - \frac{1}{n})$ = shape parameter

This type of relationship describes the hydraulic properties of the soil for any degree of saturation and to realistically simulate infiltration processes from a point source under high gradients of soil moisture.

Conceptualization of the point source emitter

Water application from the drip emitter was considered as a localized constant flux boundary condition. Due to the axial symmetry around the single point source of water, soil water flow was simulated in two dimensions with an axis of symmetry. Thus, water flow in both radial and vertical directions was considered. The lateral boundary of the domain was set as the no-flow boundary to minimize the lateral losses. On the contrary, the bottom boundary was set to drain freely to allow for gravity-induced flow of water below the simulated soil profile.

Interpretation of wetting front development

The wetted soil volume is limited by a transition zone between the wetted soil and the drier soil. In the case of field measurements, the field-surveyed wetting front is determined by visual assessment of the transition zone between the wet soil and the initially dry soil. In the case of simulation, the simulated wetting front is estimated from the simulated soil water content using a specific threshold value. Hence, the shape of the simulated wetting front is controlled by the threshold value selection. At the same time, by using this threshold value, it is possible to compare the time-based dynamics of the field observed and simulated wetting fronts. Understanding the behavior of the radial and vertical advance of wetting front created by a point source is critical to design the drip irrigation systems. The excessive downward advance may cause deep percolation while insufficient radial advance may lead to dry spots or poor two-dimensional wetting. A physically based theoretical model can provide the necessary guidelines for the emitter discharge rate, spacing and irrigation time.

Numerical model development: domain, mesh, and boundary conditions

The numerical model was formulated by considering an appropriate simulation domain and spatial discretization as well as hydraulic boundary conditions necessary to describe water flow in variably saturated porous media subjected to point source drip irrigation. Due to the symmetry of the flow field around a surface emitter, the two-dimensional (2-D) vertical cross-section was sufficient to investigate the physical process. The horizontal axis of the 2-D cross-section extended to 70 cm (i.e., −35 to +35 cm) to ensure that the lateral extent of water flow around the emitter is appropriately resolved while the vertical dimension was taken as 100 cm to capture the downward advance of the wetting front. The surface point source was located at x = 0 cm, spanning a local 2 × 1 cm region with an assigned flux boundary condition that corresponds to a constant discharge rate as applied experimentally. The domain was discretized using a finite element mesh comprising 1,543 nodes and 3,084 triangular elements (Arshad et al., 2019). A mesh refinement was applied to capture steep hydraulic gradients that develop in the vicinity of the emitter due to significant infiltration rates during the early stage of the simulation. Elements far from the source were deliberately made coarse to reduce the number of elements and computational effort (Figure 1). Hydraulic boundary conditions were primarily imposed as Neumann-type (flux-based) boundary conditions.

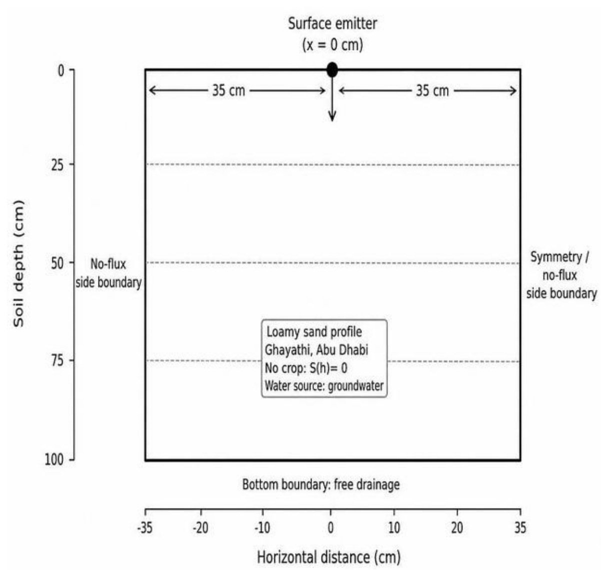

Fig. 1. Two-dimensional simulation domain, surface emitter position, and hydraulic boundary conditions.

The flux Neumann condition was applied to the surface of the emitter, representing water application at the constant rate while the two sides were set to zero-flux Neumann condition to account for symmetry (Figure 2). Finally, the bottom boundary of the domain was assigned a free drainage Neumann boundary condition to represent gravity-driven flow below the rooting zone. An atmospheric boundary condition, which takes the form of a mixed (Cauchy-type) boundary condition in HYDRUS-2D, was applied to the soil surface outside the emitter region. Because evaporation was ignored and surface ponding was prevented in this study, the boundary condition was a flux-controlled Neumann boundary condition during the entire simulation period. A fixed pressure-head (Dirichlet) boundary condition was used during the simulations. Initial conditions were established by specifying an initial pressure head that approximated the field-measured moisture content before irrigation. The initial pressure head acted as an initial condition rather than a boundary condition. Ponding at the air-soil surface was prevented to avoid numerical instabilities and to achieve a physically consistent infiltration process.

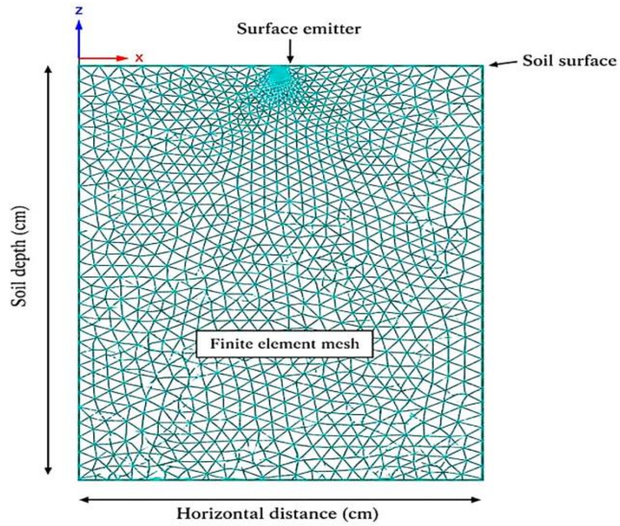

Fig. 2. General finite element mesh used in the HYDRUS-2D simulation.

Wetting front observations and model outputs

At each observation time, the surface wetted radius, surface wetted diameter, and maximum vertical wetting depth were measured manually for bare-soil experiments. Simultaneously, the corresponding HYDRUS-2D simulations were stored for these observation times to compare the observed values with the simulated data. Simulated radial and vertical wetting front positions for each time were obtained from HYDRUS-2D software by applying the same visual criterion, which was used for the manual measurements, to distinguish wet and relatively dry soil regions. Thus, using one visual criterion for HYDRUS-2D simulations allowed comparing the measured and simulated data at particular time steps.

Statistical evaluation

Agreement between the observed (O_i) and simulated (S_i) dimensions was evaluated using the mean error (ME), root mean square error (RMSE), model efficiency (EF; Nash-Sutcliffe efficiency), absolute maximum relative error (AMRE), and the coefficient of determination (R^2):

$$\text{ME} = \frac{1}{n}\sum_{i=1}^{n}(S_\text{i} - O_\text{i}) \quad (02)$$

$$\text{RMSE} = \left[\frac{1}{n}\sum_{i=1}^{n}(S_\text{i} - O_\text{i})^2\right]^{0.5} \quad (03)$$

$$\text{EF} = 1 - \frac{\sum_{i=1}^{n}(S_\text{i}-O_\text{i})^2}{\sum_{i=1}^{n}(O_\text{i}-O_\text{a})^2} \quad (04)$$

$$\text{AMRE}\ (\%) = \frac{(O_\text{o}-S_\text{s})}{O_\text{o}} \times 100 \quad (05)$$

RESULTS

Dynamics of observed wetting front advancement

The wetting front developed laterally and vertically throughout the time of irrigation. The radius of the surface wetting increased steadily from 12.0 cm at 15 min to 24.0 cm at 180 min. At the same time, the maximum depth of the vertical advance increased steadily from 16.0 cm to 74.0 cm, as shown in Table 2. Moreover, the wetting bulb showed a significant increase in vertical advance over its lateral advance throughout the infiltration process, evidenced by the increase in the depth-to-radius ratio from 1.33 to 3.08 cm. It indicates that the soil moisture moved downward under gravity, and thus, the infiltration process was controlled by gravitational forces, which is also typical for coarse-textured soils.

Table 2. Observed and simulated wetting dimensions under point source drip irrigation.

S. No.	Time (min)	Observed			Simulated		
		Surface Wetted Radius, R_{wo} (cm)	Surface Wetted Diameter, D_{wo} (cm)	Maximum Vertical Depth, Z_{wo} (cm)	Surface Wetted Radius, R_{ws} (cm)	Surface Wetted Diameter, D_{ws} (cm)	Maximum Vertical Depth, Z_{ws} (cm)
1	15	12.0	24.0	16.0	11.38	22.76	16.45
2	30	13.5	29.0	25.5	13.59	27.18	24.01
3	45	15.5	31.0	31.5	14.66	29.32	29.58
4	60	16.5	33.0	37.5	15.51	31.02	35.31
5	75	17.0	34.0	41.0	16.08	32.16	38.93
6	90	17.5	38.0	46.0	17.86	35.72	42.95
7	105	19.5	39.0	51.0	18.57	37.14	48.01
8	120	20.0	40.0	57.5	19.01	38.02	53.74
9	135	21.0	42.0	60.5	20.42	40.84	56.75
10	150	23.0	46.0	65.0	21.53	43.06	60.66
11	165	23.5	47.0	69.0	21.91	43.82	64.44
12	180	24.0	48.0	74.0	22.03	44.06	69.40

The observed and simulated results of surface wetted radius, surface diameter and maximum vertical wetting depth were similar to each other during the irrigation periods. In terms of the irrigation time, both observed and simulated wetting dimensions tended to increase, indicating that the model was able to simulate the general trend of the observed wetting front development. The comparisons of the observed and simulated data at different observation times are given in Table 2. The simulated values of wetting dimensions at later stages of irrigation were generally slightly lower than the observed ones, suggesting that the model slightly underestimated the wetting front development with the increase of the distance from the emitter.

Simulated Water Content Distributions

Simulated soil water contents were used to visualize the time-based evolution of two-dimensional wetted soil volumes around the point source. At the beginning of irrigation (15 min), large increases in soil moisture were observed only in the vicinity of the emitter (Figure 3). After 60 min of irrigation, the zone of increased soil moisture content had developed laterally reaching approximately one third of the profile depth. At 120 and 180 min, the simulated soil moisture patterns indicated a distinct downward extension of the wetted bulb with less pronounced lateral extension (Figure 4). Over the entire simulation period, the vertical profiles of soil water content were approximately symmetric distributed with respect to the centre of the emitter, which suggests that the 2-D modeling approach and the defined boundary conditions are appropriate to study the described physical process.

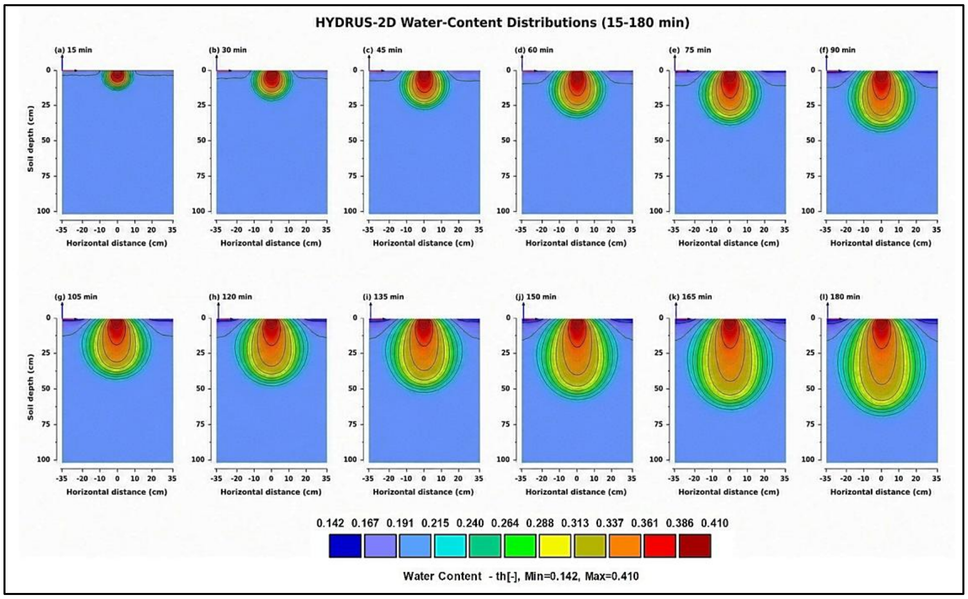

Fig. 3. Representative simulated volumetric soil water content distributions at various times.

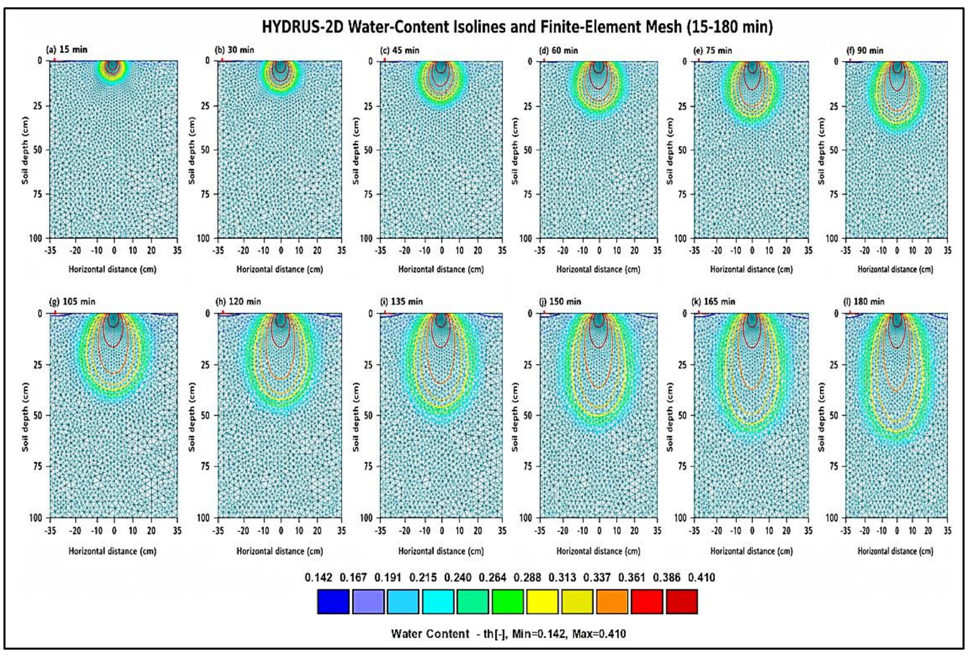

Fig. 4. Simulated soil water content isolines and finite element mesh at various time intervals.

Model prediction of surface wetted radius

The time-based pattern of the simulated surface wetted radius was close to the field observations shown in (Figure 5). The simulated values gradually increased from 11.38 cm at 15 min to 22.03 cm at 180 min while the observed data varied between 12.0 and 24.0 cm. An overestimation was observed at 30 and 90 min while underestimation dominated at later simulation times. The statistical analysis of surface wetted radius showed that the model exhibited a mean error (ME) of -0.87 cm, root mean square error (RMSE) of 1.07 cm, a model efficiency (EF) of 91.80 %, and an absolute maximum relative error (AMRE) of 8.21 %. The regression analysis of observed versus simulated values showed a strong linear agreement (R^2 = 0.981) with a slope of 0.885, an intercept of 1.258 cm, and a slight underestimation at higher values (Figure 5).

Table 3. Observed (Rwo) and simulated (Rws) surface wetted radius with associated error, squared error, squared deviation, and relative error used for statistical evaluation of model performance.

S. No	Observed surface wetted radius	Simulated surface wetted radius	Error	Squared Error	Squared Deviation	Relative Error
	Rwo	Rws	$(R_{wsi} - R_{woi})$	$(R_{wsi} - R_{woi})^2$	$(R_{woi} - R_{wa})^2$	$= \frac{(R_{wo} - R_{ws})}{R_{wo}} \times 100$
	(cm)	(cm)	(cm)	(cm^2)	(cm^2)	(%)
1	12	11.38	-0.62	0.38	43.34	5.17
2	13.5	13.59	0.09	0.01	25.84	-0.67
3	15.5	14.66	-0.84	0.71	9.51	5.42
4	16.5	15.51	-0.99	0.98	4.34	6.00
5	17	16.08	-0.92	0.85	2.51	5.41
6	17.5	17.86	0.36	0.13	1.17	-2.06
7	19.5	18.57	-0.93	0.86	0.84	4.77
8	20	19.01	-0.99	0.98	2.01	4.95
9	21	20.42	-0.58	0.34	5.84	2.76
10	23	21.53	-1.47	2.16	19.51	6.39
11	23.5	21.91	-1.59	2.53	24.17	6.77
12	24	22.03	-1.97	3.88	29.34	8.21

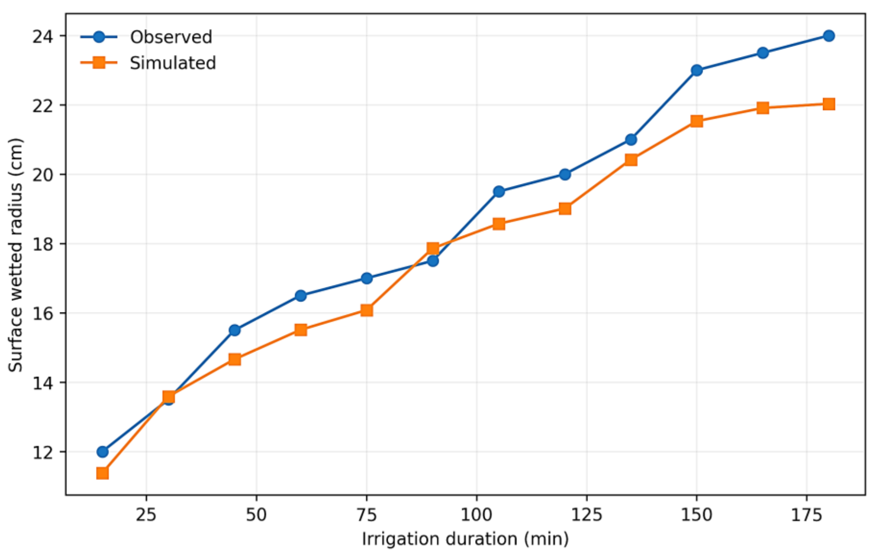

Fig. 5. Comparison of observed and HYDRUS-2D simulated surface wetted radius as a function of irrigation duration.

Model prediction of maximum vertical wetting depth

Simulated maximum vertical wetting depth increased from 16.45 cm at 15 min to 69.40 cm at 180 min, while the observed vertical depths increased from 16 cm to 74 cm, as given in Table 4 and shown in Figure 6. There is an apparent overestimation of simulated results just at the first moment, while an underestimation occurred in later periods. Performance statistics for vertical wetting depth indicated an ME of -2.86 cm, RMSE of 3.19 cm, EF of 96.62 %, AMRE of 6.68 %, and R^2 of 0.997. Despite the larger RMSE relative to surface radius, the high model efficiency reflects excellent predictive performance across the broader range of observed vertical wetting depths.

Table 4. Observed (Zwo) and simulated (Zws) maximum vertical depth with associated error, squared error, squared deviation, and relative error used for statistical evaluation of model performance.

S. No	Observed Maximum Vertical Depth Zwo (cm)	Simulated Maximum Vertical Depth Zws (cm)	Error $(Z_{wsi} - Z_{woi})$ (cm)	Squared Error $(Z_{wsi} - Z_{woi})^2$ (cm^2)	Squared Deviation $(Z_{woi} - Z_{wa})^2$ (cm^2)	Relative Error $= \frac{(Z_{wo} - Z_{ws})}{Z_{wo}} \times 100$ (%)
1	16	16.45	0.45	0.20	1016.02	-2.81
2	25.5	24.01	-1.49	2.22	500.64	5.84
3	31.5	29.58	-1.92	3.69	268.14	6.10
4	37.5	35.31	-2.19	4.80	107.64	5.84
5	41	38.93	-2.07	4.28	47.27	5.05
6	46	42.95	-3.05	9.30	3.52	6.63
7	51	48.01	-2.99	8.94	9.77	5.86
8	57.5	53.74	-3.76	14.14	92.64	6.54
9	60.5	56.75	-3.75	14.06	159.39	6.20
10	65	60.66	-4.34	18.84	293.27	6.68
11	69	64.44	-4.56	20.79	446.27	6.61
12	74	69.4	-4.6	21.16	682.52	6.22

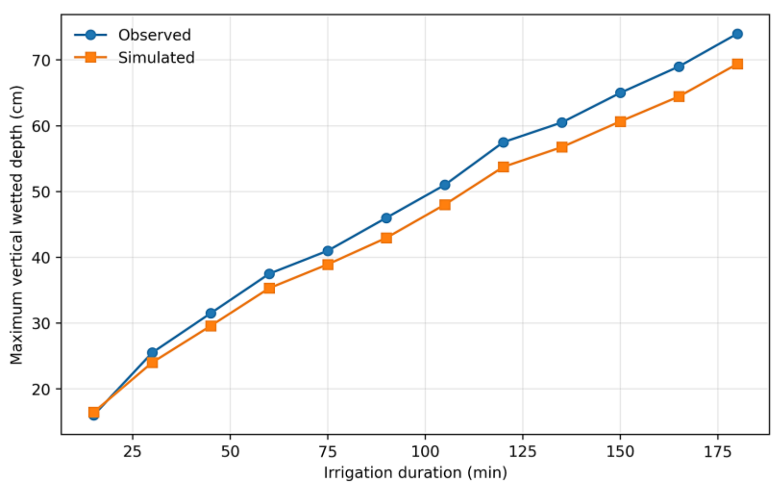

Fig. 6. Comparison of observed and HYDRUS-2D simulated maximum vertical wetted depth as a function of irrigation duration.

Summary of model performance indicators

The performance of the models was evaluated using the mean error (ME), root mean square error (RMSE), model efficiency (EF), maximum absolute relative error (AMRE), and coefficient of determination (R^2). These statistical measures indicate the accuracy and consistency of the predicted results. Table 5 summarizes the statistical comparison of observed and simulated values of the wetting dimensions. Both the ME values of surface wetted radius and maximum vertical depth were slightly negative, implying that the simulated results were generally underestimated. This underestimation was relatively small, as indicated by the negative sign of ME. The RMSE values represent the magnitude of the error and indicate the deviation of the simulated values from the measured values.

A small RMSE indicates that the measured and predicted values of soil moisture were close to each other. On the other hand, RMSE does not indicate whether the model tends to underestimate or overestimate the observations. For both model outputs, the ME and RMSE values were small, suggesting that HYDRUS 2D has excellent predictive performance for the wetting front of point source drip irrigation in loamy sand. Finally, the model efficiencies (EF) were more than 90%, which indicates that HYDRUS 2D can accurately predict wetting front advances under a point water source with minimal error for both wetting dimensions in loamy sand soil. In addition to the statistical characteristics, another criterion for the model's verification is the analysis of the dependence of the calculated dimension of wetting on the observed values by means of a log-log regression (Figure 7).

Table 5. Statistical indicators of model performance.

Variable	ME (cm)	RMSE (cm)	EF (%)	AMRE (%)	R^2
Surface wetted radius	-0.87	1.07	91.80	8.21	0.981
Maximum vertical depth	-2.86	3.19	96.62	6.68	0.997

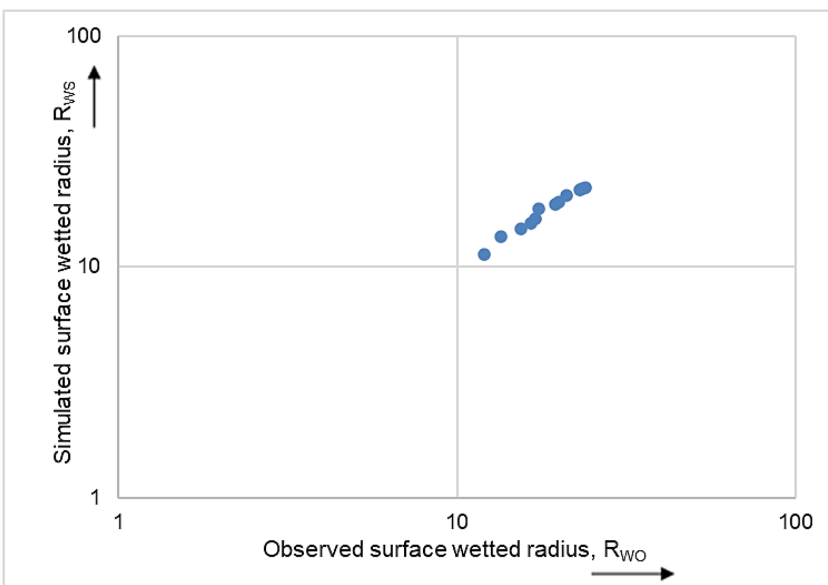

Fig. 7. Log-log relationship between observed and simulated surface wetted radius for model evaluation.

The log-log plot of the surface radius demonstrates a possibility of the regression line with a slope close to 1, which indicates the absence of systematic error in the calculations for both small and large values of the radius. Similar results are obtained for the vertical axis for the maximal depth of wetting (Figure 8). Moreover, statistical measures combined with log-log analysis indicate that the model's agreement with observations is good for both small and large wetting fronts. This suggests that the discrepancies identified between observations and simulations are relatively minor and do not change significantly with the considered wetting front size. All of these results together suggest that the numerical model is indeed capable of accurately predicting both radial and vertical wetting front advances for point source drip irrigation and can be used for this type of prediction.

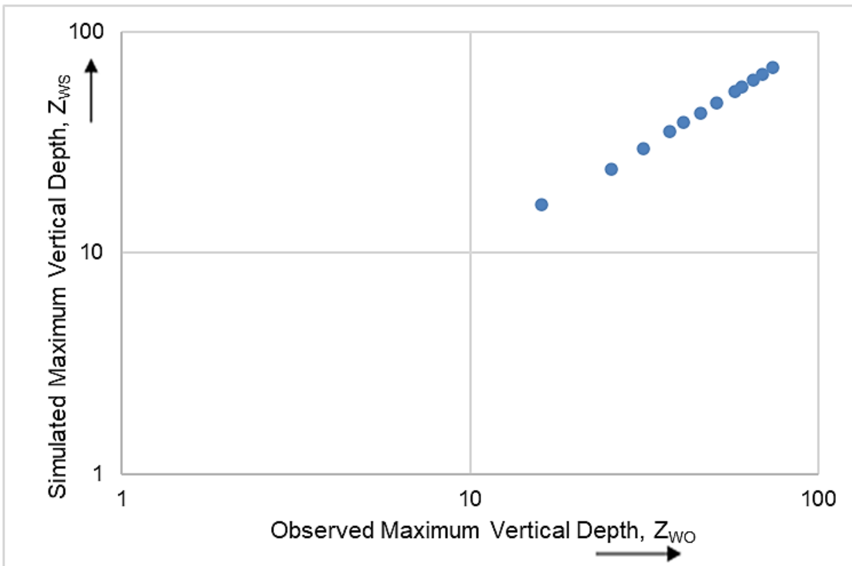

Fig. 8. Log-log relationship between observed and simulated maximum vertical wetted depth for model evaluation.

DISCUSSION

The measured and simulated wetting dimensions obtained in this study help understand the behavior of a point source drip irrigation system in the case of coarse textured bare soil. The surface wetted diameter reached 48 cm while the front advanced vertically to 74 cm deep after 180 min. Thus, these results indicate that for such a type of soil, mainly due to its high conductivity and low field capacity, the irrigation process under continuous operation leads to preferential flow of infiltrated water downwards rather than laterally as is the case of the loamy sand. In agricultural practice, this result implies that for obtaining surface overlap for the same crop with similar irrigation time, the emitter spacing should be equal or smaller than the surface wetted diameter. However, in the selection of emitter spacing, other factors, such as root systems distribution, irrigation time, and soil hydraulic properties, should also be taken into account since they can greatly affect the wetted root zone dimensions (Shabani *et al.,* 2024).

The significant vertical wetting obtained in this study has implications for irrigation practices in arid regions. A depth of 74 cm is excessive for many horticultural or young perennial crops, therefore resulting in losses due to deep percolation. Similar considerations have been made in recent drip irrigation studies, noting that adjustments in the duration or frequency of irrigation may be more effective in coarse textured soils than changes in discharge rate

(Alhammadi and Al Shrouf, 2013). These include drip irrigation with shorter irrigation times, lower application rates or even intermittent (pulsed) irrigation to maintain higher percentages of applied water in the root zone.

The statistical parameters obtained in this study indicate that HYDRUS 2D model is capable of simulating both radial and vertical wetting front developments with high efficiency. The model efficiency values and coefficient of determination were found to be high, which implies that the time-based changes in wetting characteristics were reproduced reasonably well by the simulations. However, it is evident that with the increase in wetting front size, the model slightly underestimates the values, which might be due to systematic error. This might be explained by the fact that in HYDRUS 2D, the depth-averaged hydraulic properties are used to describe the vertically differentiated soil profile (Shiri *et al.,* 2020; Rasoulzadeh *et al.,* 2025). Besides, small deviations may be caused by the fact that the point source was used to simulate the emitter while in practice a particular pattern of wetting front is formed. In addition, there might be a possibility that the visual estimation of the wetting front differed from the particular location, which was used in the simulation as a wetting front.

Regardless of this limitation, the near unity obtained in all log-log regressions suggests that model prediction errors were not proportional to the absolute value of the measured wetting dimensions. This implies that the accuracy in estimating both shallow and deep wetting is adequate and supports the validity of the approach used. HYDRUS-based simulation of drip irrigation has also been recently reviewed, with similar conclusions on the reliability of model performance in the studies by (Morianou *et al.*, 2023).

The progressive increase in the depth to radius ratio observed in both measured and modeled observations can be explained by the transition in dominant flow mechanism during irrigation. Steep pressure head gradients in the immediate vicinity of the emitter during the early stages resulted in more extensive spreading of moisture through capillary forces in multiple directions. As irrigation progressed, the dominant mechanism switched to gravitational flow, resulting in deep elongation of the wetting bulb in the vertical direction. Similarly to recent numerical studies, the results of this study indicate that coarse textured soils tended to have deeper and narrower wetted bulb than finer textured soils for the same cumulative infiltration volume (Li *et al.,* 2023). The agreement between measured and predicted wetting patterns indicates that our model captured the main physical processes responsible for redistribution of water from a point source under drip irrigation.

The numerical model presented in this study is appropriate to facilitate irrigation design and management decisions by avoiding time consuming field experiments. The model can predict wetting dimensions for a particular discharge and a particular soil, which in turn can help to establish initial ideas about emitter spacing, irrigation time, and application method. At the same time, the latest trends in agricultural engineering suggest that successful drip irrigation schemes should be designed using numerical modeling combined with crop-root system, soil and irrigation schedules analyses (Vishwakarma *et al.,* 2023). Thus, the findings of this study can be used as a starting point for further calculations involving different discharge rates, initial soil moisture contents, and pulsed irrigation regimes.

CONCLUSION

This study showed that surface point source drip irrigation method in loamy sand soil generated a mainly vertical soil water distribution pattern. At 180 min after the irrigation initiation, the depth of the wetting front (74 cm) was significantly greater than the diameter (48 cm). Due to a high infiltration capacity of loamy sand, drip irrigation with long irrigation time may lead to significant deep percolation losses. HYDRUS-2D model was able to simulate the time-based variation of both the radial and vertical soil water contents with high accuracy. The model's efficiency was high in all cases, with an average model efficiency of more than 90%, while the root mean square error (RMSE) was reasonably low, and the coefficient of determination was higher than 0.98 for both the depth and diameter of the wetting front. However, the model slightly underestimated the observed depth and diameter of the wetting front, which might be seen in the negative mean error values. The study has shown that the HYDRUS-2D model is an efficient tool for simulating the wetting pattern of point source drip irrigation in arid loamy sand. The model can be used in practice for optimizing the drip irrigation systems, including determining the emitter spacing and irrigation time. In case of coarse texture soil, it is needed to limit the irrigation time or arrange the irrigation process periodically to avoid excessive deep percolation.

CONFLICT OF INTEREST

The authors hereby declare that they have no conflict of interest.

Generative AI statement

The author(s) declare that no Generative AI was used in the creation of this manuscript.

Publisher's note

All claims expressed in this article are solely those of the authors and do not necessarily represent those of their affiliated organizations, or those of the publisher, the editors, and the reviewers. The publisher does not guarantee or endorse any product that may be reviewed in this article or any claim made by its manufacturer.

REFERENCES

Alhammadi, M.S., Al-Shrouf, A.M., 2013. Irrigation of sandy soils: Basics and scheduling. In: Crop Production. Intech Open. https://doi.org/10.5772/55117

Al-Ogaidi, A.A.M., Wayayok, A., Rowshon, M.K., Abdullah, A.F., 2016. Wetting patterns estimation under drip irrigation systems using an enhanced empirical model. Agric. Water Manag., 176: 203–213. https://doi.org/10.1016/j.agwat.2016.06.002

Arshad, I., Babar, M.M., Vallejera, C.A., 2019. Computation of Seepage and Exit Gradient through a Non-Homogeneous Earth Dam without cut-off walls by using Geo-Slope (SEEP/W) Software. PSM Biol. Res., 4(1): 40-50.

Cook, F.J., Thorburn, P.J., Fitch, P., Bristow, K.L., 2003. WetUp: A software tool to display approximate wetting patterns from drippers. Irrig. Sci., 22: 129–134. https://doi.org/10.1007/s00271-003-0078-2

Cote, C.M., Bristow, K.L., Charlesworth, P.B., Cook, F.J., 2003. Analysis of soil wetting and solute transport in subsurface trickle irrigation. Irrig. Sci., 22: 143–156. https://doi.org/10.1007/s00271-003-0080-8

Fan, Y., Zhang, C., Tang, X., Shi, J., Liang, J., 2023. An improved dimensional model for calculating the wetting pattern in soil under drip irrigation. J. Irrig. Drain. Eng., 149(9): 04023033. https://doi.org/10.1061/JIDEDH.IRENG-9993

Kandelous, M.M., Šimůnek, J., 2010. Comparison of numerical, analytical, and empirical models to estimate wetting patterns for surface and subsurface drip irrigation. Irrig. Sci., 28: 435–444. https://doi.org/10.1007/s00271-009-0205-9

Li, Y., Nie, W.B., Feng, Z.J., 2023. Development of a soil wetting pattern estimation model for drip irrigation. Water Supply., 23(1): 144–161. https://doi.org/10.2166/ws.2022.429

Morianou, G., Kourgialas, N.N., Karatzas, G.P., 2023. A review of HYDRUS-2D/3D applications for simulations of water dynamics, root uptake and solute transport in tree crops under drip irrigation. Water., 15(4): 741. https://doi.org/10.3390/w15040741

Mualem, Y., 1976. A new model for predicting the hydraulic conductivity of unsaturated porous media. Water Resour. Res., 12: 513–522. https://doi.org/10.1029/WR012i003p00513

Naglič, B., Kechavarzi, C., Coulon, F., Pintar, M., 2014. Numerical investigation of the influence of texture, surface drip emitter discharge rate and initial soil moisture condition on wetting pattern size. *Irrig. Sci*, 32: 421–436. https://doi.org/10.1007/s00271-014-0439-z

Rasoulzadeh, A., Kohan, M.R., Amirzadeh, A., et al. 2025. Improving soil water simulation in semi-arid agriculture: A comparative evaluation of water-retention curves and inverse modeling using HYDRUS-1D. Hydrol., 12(10): 273. https://doi.org/10.3390/hydrology12100273

Richards, L.A., 1931. Capillary conduction of liquids through porous mediums. Phys., 1: 318–333. https://doi.org/10.1063/1.1745010

Schwartzman, M., Zur, B., 1986. Emitter spacing and geometry of the wetted soil volume. J. Irrig. Drain. Eng., 112: 242–253. https://doi.org/10.1061/(ASCE)0733-9437(1986)112:3(242)

Shabani, A., Sepaskhah, A.R., Golestani, M., Shahabi Zad, V., 2025. Use of dimensionless time and water volume to estimate subsurface drip irrigation wetted zone in different soil textures. Sci. Rep., 15: 23971. https://doi.org/10.1038/s41598-025-07841-6

Shiri, J., Karimi, B., Karimi, N., Kazemi, M.H., Karimi, S., 2020. Simulating wetting front dimensions of drip irrigation systems: Multi-criteria assessment of soft computing models. J. Hydrol., 585: 124792. https://doi.org/10.1016/j.jhydrol.2020.124792

Skaggs, T.H., Trout, T.J., Šimůnek, J., Shouse, P.J., 2004. Comparison of HYDRUS-2D simulations of drip irrigation with experimental observations. J. Irrig. Drain. Engin., 130: 304–310. https://doi.org/10.1061/(ASCE)0733-9437(2004)130:4(304)

Šimůnek, J., van Genuchten, M.Th., Šejna, M., 2016. Recent developments and applications of the HYDRUS computer software packages. Vadose Zone J., 15: 1–25. https://doi.org/10.2136/vzj2016.04.0033

van Genuchten, M.Th., 1980. A closed-form equation for predicting the hydraulic conductivity of unsaturated soils. Soil Sci. Soc. Am. J., 44: 892–898. https://doi.org/10.2136/sssaj1980.03615995004400050002x

Vishwakarma, D.K., Kumar, R., Tomar, A.S., Kuriqi, A., 2023. Eco-hydrological modeling of soil wetting pattern dimensions under drip irrigation systems. Heliyon, 9(7): e18078. https://doi.org/10.1016/j.heliyon.2023.e18078

Zur, B., 1996. Wetted soil volume as a design objective in trickle irrigation. Irrig. Sci., 16: 101–105. https://doi.org/10.1007/BF02215617